한국공작기계학회논문집 Vol.17 No.4 2008. 8.
Transactions of the Korean Society of Machine Tool Engineers

Pareto Optimal Design of the Vehicle Body

Byoung-Gon Kim*, Tae-Jin Chung*, Jeong-Ick Lee+

(논문접수일 2008. 2. 20, 심사완료일 2008. 4. 21)

차체의 팔렛토 최적 설계

김병곤*, 정태진*, 이정익+

Abstract

The important dynamic specifications in the aluminum automobile body design are the vibrations and crashworthiness in the views of ride comforts and safety. Thus, considerable effort has been invested into improving the performance of mechanical structures comprised of the interactive multiple sub-structures. Most mechanical structures are complex and are essentially multi-criteria optimization problems with objective functions retained as constraints. Each weight factor can be defined according to the effects and priorities among objective functions, and a feasible Pareto-optimal solution exists for the criteria-defined constraints. In this paper, a multi-criteria design based on the Pareto-optimal sensitivity is applied to the vibration qualities and crushing characteristics of front structure in the automobile body design. The vibration qualities include the idle, wheel unbalance and road shake. The crushing characteristic of front structure is the axial maximum peak load.

Key Words : DOE(design of experiments)(실험설계), RSM(response surface method)(응답 표면법), Pareto optimum solution(팔렛토 최적해), multi-criteria(다 기준), aluminum-intensive body(알루미늄 인텐시브 바디)

Notation

X	Design variable set
$F(X)$	Weighted objective function
w_i	Weighting factor of i-th objective fn.
$L(\cdot)$	Lagrange function
S	Search direction vector
λ	Lagrange multipliers of constraints
μ	Lagrange multipliers of normalized search direction constraint

* 군산대학교 기계공학과
+ 교신저자, 인하공업전문대학 기계설계과 (jilee@inhatc.ac.kr)
주소: 402-752 인천광역시 남구 용현동 253번지

1. Introduction

Most of applications of aluminum materials are made in the chassis and body component designs. Auto-makers have doubled the aluminum used in the vehicles since 1991 and predict that their applications will be up to 50 percent in next five years. The design of aluminum-intensive automobile body such as general structural designs of automotive bodies is similarly subject to both structural performance specifications, like strength and stiffness and to cost.

Thus, a structural design for a minimum weight structure with maximum performance, under the given constraints may be needed from the concept design stage. These types of optimization are based on the assumption that the geometry of the structure is defined by its boundaries, and that an optimal design can be found by varying the design variables. In practical applications, there are also interactions among different criteria and objective functions. Thus, a Pareto-optimal solution is needed. Considerable research evaluating the design of automotive body structure has been undertaken and this will likely continue in order to improve design efficiency[5~10].

This paper deals with the design development process of the aluminum intensive body through system engineering approaches. The detailed design consideration presents a multi-criteria optimization design based on a Pareto-optimal sensitivity for the vibration and crashworthiness specifications as the multiple specifications[1~5]. For the usable and feasible initial design parameters, the DOE/RSM approach is used. In the DOE/RSM approach, the objective when optimizing a design process is to select a combination of control factors as the process condition that meet manufacturability and performance specifications. Using design of experiment (DOE) combined with response surface methodology (RSM) is a effective strategy that can examine the whole design parameter space. The initial step is to perform some computer-based screening experiments that identify the important control factors.

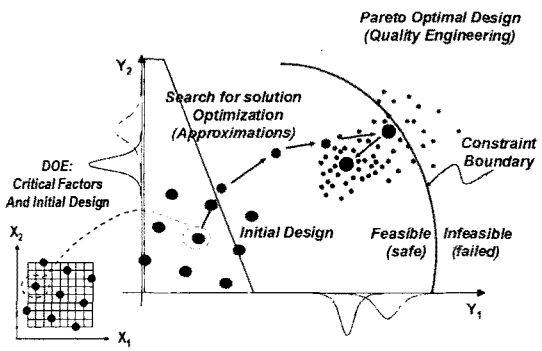

Fig. 1 Overall design strategies

2. Pareto-optimal solution in the multicriteria structural specifications

Mathematically, the objective and constraint functions of a given problem are separable in the design variables x_i so that the inequality-constrained problem can be stated as.

Find $X=\{x_1\ x_2\ \cdots\ x_m\}^T$ which minimizes

$$F(X)=\sum_{i=1}^{n} f_i(X) \tag{1}$$

subject to $g_j(X)\le 0,\ j=1,\ldots,k$ (2)

For solving a sequence of problems, a weighting method is needed in which the objective is defined by a linear combination of all objective functions with non-negative weighting factors. Thus, the objective function, $F(X)$, can be redefined by:

$$F(X)=\sum_{i=1}^{n} w_i\, f_i(X) \tag{3}$$

where the weighting factors w_i are normalized so that $\sum_{i=1}^{n} w_i = 1$.

This problem can be solved by the method of Lagrange multipliers; we can construct the Lagrange function L as:

$$L(X,\lambda,w)=\sum_{i=1}^{n} w_i\, f_i(X)+\sum_{j=1}^{k}\lambda_j\, g_j(X) \tag{4}$$

where $\lambda = \{\lambda_1 \lambda_2 ... \lambda_k\}^T$ is the vector of the Lagrange multipliers.

The stationary points of the Lagrange function can be found by solving the following equations from the Kuhn-Tucker optimality condition:

$$\frac{\partial L(X,\lambda,w)}{\partial x_i} = \sum_{i=1}^{n} w_i \frac{\partial f_i(X)}{\partial x_i} + \sum_{j=1}^{k} \lambda_j \frac{\partial g_j(X)}{\partial x_i} = 0 \quad (5)$$

$$\frac{\partial L(X,\lambda,w)}{\partial \lambda_i} = g_j(X) = 0 \quad (6)$$

In general, no solution vector X exists that minimizes all n objective functions simultaneously. Hence, so-called Pareto-optimal solutions are sought in multi-objective optimization problems. A feasible solution X^* is called Pareto-optimal if there exists no other feasible solution X such that $f_i(X) \le f_i(X^*)$ for $i = 1,...,n$. In other words, a feasible vector X^* is called Pareto optimal if there is no other feasible solution that would reduce some objective function without causing a simultaneous increase in at least one other objective function. In the global criterion method, the optimal solution X^* is found by minimizing a pre-selected global criterion $F(X)$, such as the sum of the squares of the relative deviations of the individual objective functions from the feasible solutions. Thus X^* is formed by minimizing

$$F(X) = \sum_{i=1}^{n} \left(w_i \frac{f_i(X^*) - f_i(X)}{f_i(X^*)} \right)^p \quad (7)$$

subject to $g_j(X) \le 0$, $j = 1,...,k$

where p is a constant and X^* is the ideal solution for the objective function. The solution X^* is obtained by minimizing $f_i(X)$ subject to the constraints $g_j(X) \le 0$. If a feasible solution X^* is the Pareto optimum of eq. (1) and (2), then there exist multipliers $\lambda_j \ge 0$, $j = 1,...,k$ and $w_i \ge 0$, $i = 1,...,n$.

3. Simulation

As an example, the dynamic characteristics of an automotive body were simulated for the frequency response of body and crushing quality of rail front. Frequency response is one of the most important factors influencing the overall NVH quality of a passenger vehicle. In particular, the driver is sensitive to the vibrations of the steering wheel in the frequency range of engine idle shake, wheel shake, and road shake. By controlling these kinds of vibrations and understanding the current phenomena in more detail, a well-correlated finite-element model can be found. Although deciding what the variables are is relatively simple, deciding how to apply them to a realistic model is a different problem in terms of feasibility and reliability. To obtain a reliable model, a total vehicle model with main components shown in Figure 2 was validated with test results as shown in Table 1. The body system, suspension system, exhaust system and steering system are shown in figure 3 as the chassis system attached to the body-in-white. The correlation between the detailed model and the hybrid simple model was validated by Modal Assurance Criteria (MAC) in eq. (8). MAC values in the range of frequencies appear to be more than 80% and this model is available for a feasible vehicle design study.

$$MAC_{jk} = \frac{\left| \phi_{tj}^T \phi_{ak} \right|^2}{\left(\phi_{ak}^T \phi_{ak} \right)\left(\phi_{tj}^T \phi_{tj} \right)} \quad (8)$$

This simulation modeled the vibration characteristics with respect to engine idle shake, wheel shake, and road

Table 1 Modal assurance criteria of updated vehicle model

Reference frequency range (TEST)	Verification frequency range (FEM)	MAC Value ($j = k$)
19.34	20.38	0.93
22.55	24.52	0.92
25.38	28.22	0.89
28.96	30.81	0.94
33.74	35.52	0.95
36.99	40.21	0.92
42.01	45.18	0.93

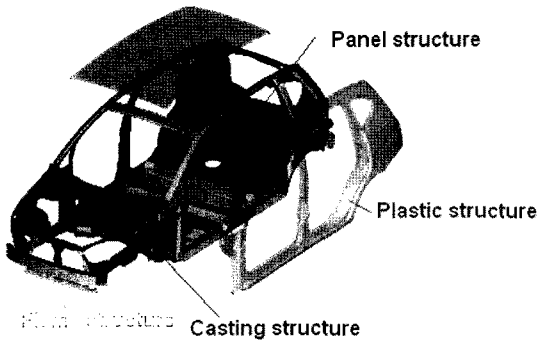

Fig. 2 Schematics of aluminum-intensive body

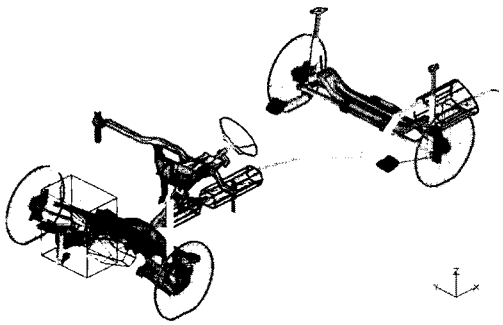

Fig. 3 Chassis system with suspension, exhaust and steering system

shake. Engine excitation can be divided into two components: the unbalanced force due to the vertical force of the piston, and the torque fluctuation due to pressure within the cylinders and the rotational moment.

For the unbalanced force, we have:

$$F = 4\left(m_{piston} + m_{conrod}\right)\frac{R^2\omega^2}{L^2}\cos 2\omega t \tag{9}$$

For torque fluctuation, we have:

$$M = -2\left(m_{piston} + m_{conrod}\right)\omega^2 R^2 \sin 2\omega t \tag{10}$$

where m_{piston} and m_{conrod} are the piston mass and connecting rod mass, R is the crank radius, L is the connecting rod length, ω is the angular velocity.

The excitations of wheel unbalance shake acted on the LH and RH front wheels with an unbalanced mass of 60 g:

$$F = M\, r\, \omega^2 \tag{11}$$

where M is the unbalanced mass of the tire wheel, r is the radius of the wheel rim and ω is the angular velocity of the wheel.

Road shake is formulated as the excitation from the running road profile, which is a force amplitude applied at the hub vertically.

$$F = C / freq^n \tag{12}$$

where C and n are 353.84 and 0.7120543, respectively. They are correlated from the running test.

To analyze the dynamic stiffness of the vehicle body, sinusoidal forces were applied at the engine excitation point and the wheel rims. The accelerations of the steering wheel and body C.G. point were calculated in the frequency range of 0~800 RPM. The multi-criteria optimization of panel thickness, average bush stiffness, and floor panel bead were performed for increasing dynamic stiffness. The damping ratio was set at3%for the frequency range of interest. The optimization problem was to find the panel thickness, floor panel bead dimensions, and average bush stiffness that minimizes initial acceleration under a given frequency range, which includes the excitation by idle shake (f_{idle}), wheel shake (f_{wheel}), and road shake (f_{road}). Beaded floor panels have been widely incorporated into automotive designs to improve dynamic stiffness[6,7]. The floor panel is designed to minimize its local deformation in the desired frequency range. Shape and sizing optimizations were simultaneously performed for the bead dimensions and panel thicknesses. Figure 4 shows bead parameters built on a flat floor: $W0$

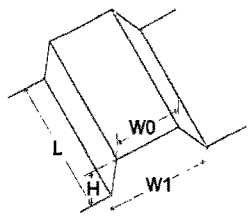

Fig. 4 Definitions of bead parameters

and $W1$ are the bead's base and top width, respectively, and H and L are the bead's height and length, respectively. Besides NVH, the crashworthiness is important item in evaluating the dynamic characteristics of structural members. In order to assess the crashworthiness and energy absorbing capacity of a structure under quasi-static or dynamic loading, it is often necessary to know the largest deflection, deformed shape and partition of energy dissipation in the structure. In the impact deformation, the elastic parameters can give the reasonable and reliable estimates for the deformation and energy absorbing properties. Using these parameters, it is often important to assess the load to initiate collapse for the stability of the section structure[8-11]. The axial maximum peak loads for a stable folding mode causing the energy absorption can be approximated from the results of tests. The axial maximum peak load (P_m) of the rectangular type member is dependent on the average edge length (C), thickness (t), yielding strength (σ_y) and Young's modulus (E) and can be written as follows[10].

$$\frac{P_m}{\sigma_y t^2} = K\left(\frac{C}{t}\right)^n, \quad K = f(\beta), \quad \beta = \frac{C}{t}\sqrt{\frac{\sigma_y}{E}} \tag{13}$$

The maximum crippling load coefficient K was approximated to $n=1.9$ through the deformation test of aluminum extruded members, as shown in figure 7 and the maximum peak load of rectangular type member can be given by.

$$K = 0.2799\,\beta^{-1.1289} \tag{14}$$

The buckling mode is dependent with the geometric dimensions and the rotational angle under the maximum bending moment can be written as the shape factor of section.

$$\frac{\theta_{\max}}{L} = 10941 \cdot \mu^{-1.533} \tag{16}$$

where $\theta_{\max}$ and L are the rotational angle and length of member under the maximum bending moment. a is the width of section, b is the height of section and t is the thickness of section. The shape factor of section (μ) in the rectangular type member is important and can be given by.

$$\mu = \frac{\sqrt[4]{a^3 b}}{t}$$

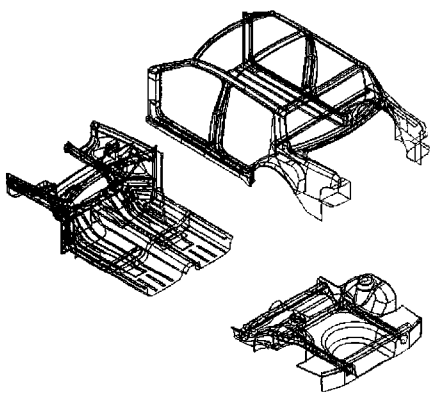

Fig. 5 Schematics of sub-structure

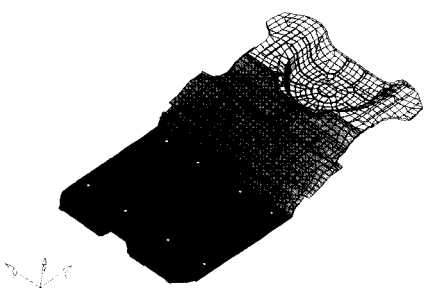

Fig. 6 Beaded floor panel

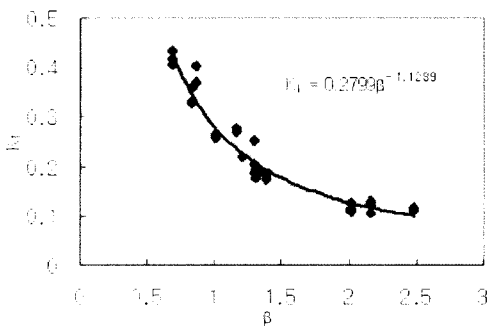

Fig. 7 Relationship of beta and maximum crippling load coefficient

The available design variables were 16 panel thicknesses, 13 beads on the floor, 2 imperfections on the rail front and 3 average bush stiffness. Figure 6 shows the beaded floor panel made through multi-criteria optimization. Table 2 shows the design variables of the initial and optimized designs. Table 3 shows the Pareto-optimal solutions obtained by weighting the design factors. Figure 7 shows the

Table 2 Design variables in initial and optimization design

Design variables	Initial design	Optimum design
Dash cross member	2.50	2.85
Dash panel	2.20	2.85
Front rail BRKT at dash	2.40	2.35
Shock tower front UPR	2.35	2.20
Shock tower LWR	2.35	2.50
Assy rail front outer	2.50	2.50
Assy rail front inner	2.50	2.80
Fender support rail	2.80	2.00
Hinge pillar INR	2.80	2.50
Hinge pillar OTR	2.00	2.55
Front rail	2.20	2.35
Skirt	1.65	1.85
Steering column SPRT BRKT	2.60	2.85
Steering column SPRT BAR	3.00	3.20
Engine MTG bush stiffness, LH	170	159
Engine MTG bush stiffness, RH	160	125
Engine MTG bush stiffness, RR	160	120
Front floor panel	2.85	2.65
Rear floor panel	2.85	2.75

Table 3 Pareto-optimal solutions

Weighting				Body weight (kg)	Weighted average acceleration (m/s^2)	Average crush force ratio (%)
w_1	w_2	w_3	w_4			
0.20	0.00	0.60	0.20	260.1	0.22	75
0.00	0.20	0.20	0.60	289.3	0.20	88
0.10	0.10	0.25	0.55	281.3	0.15	89
0.30	0.20	0.30	0.20	254.4	0.13	87
0.25	0.25	0.25	0.25	243.5	0.12	98
0.20	0.30	0.30	0.20	240.5	0.11	95
0.15	0.35	0.35	0.15	270.5	0.18	89
0.25	0.40	0.15	0.20	285.2	0.19	83
0.45	0.25	0.15	0.15	286.4	0.26	84
0.60	0.20	0.20	0.00	280.7	0.29	78
0.55	0.25	0.10	0.10	271.5	0.39	63
0.20	0.60	0.00	0.20	272.4	0.43	65

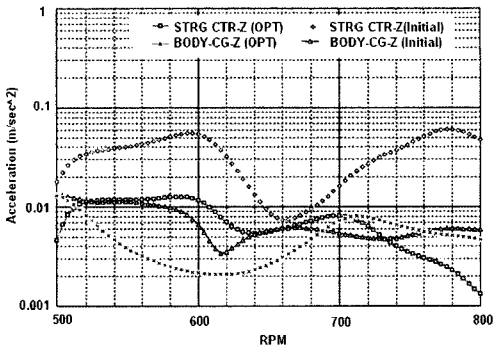

(a) Under engine idle shake

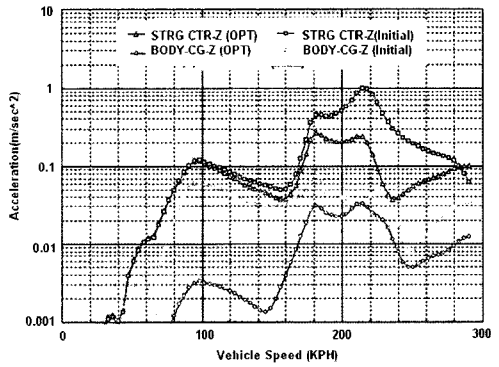

(b) Under wheel shake

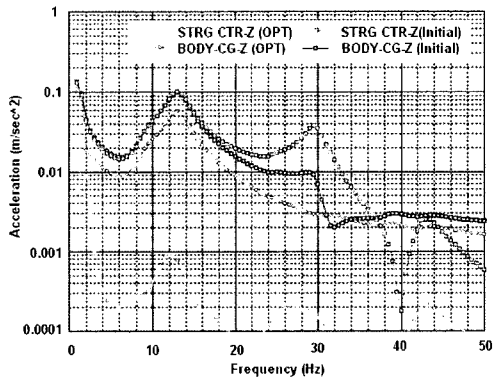

(c) Under road shake

Fig. 8 Acceleration curves of steering wheel and body C.G.

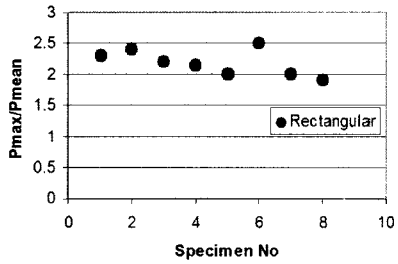

(a) Ratio of dynamic to static crush force

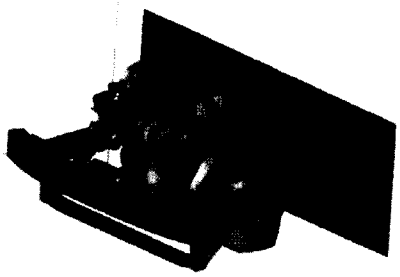

(b) Crash model for front end module

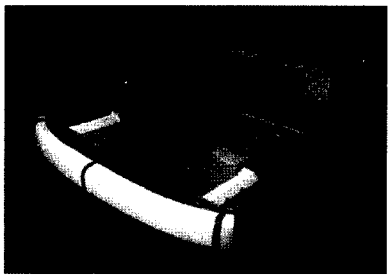

(c) Test model of front end module

Fig. 9 Simulation and test for front side rail

relationship of beta and maximum crippling load coefficient. Figure 8 shows the acceleration at the steering center and the body CG. Figure 9 shows the relative average crush force of front side rail relative to the baseline, the simple impact simulation and test model of front side rail. Figure 10 shows the manufactured aluminum body.

4. Conclusions

This paper presents the optimization design process in order to secure the structural rigidities and lightweight of weight-reduced structure. The optimum design of these

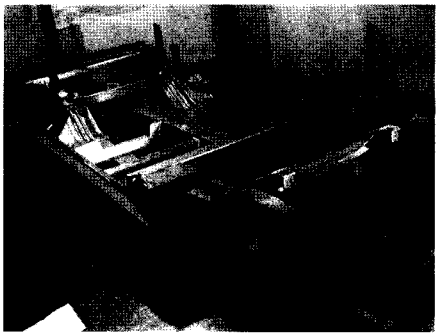

(a) Under-body model

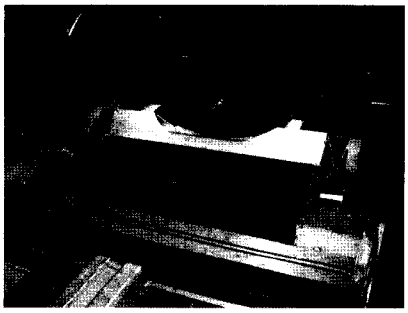

(b) Rear part component

Fig. 10 Manufactured aluminum intensive bodies

kinds of structures is very difficult to be predicted since the structural stiffness changes dramatically with the curvature and profile of reinforcement. The initially structural topology is pre-determined by topology optimization, the geometric profiles are designed by the shape optimization, and the physical dimensions such as panel's thickness and mounting location are performed by sizing optimization. The detailed explanations are as followings.

(1) For the reinforcement of the geometric dimensions of the panel or casting structures of aluminum body, the topological distributions of structural reinforcement were determined by topology optimization and more detailed dimensions of panel thickness and mounting location were designed by shape and sizing optimization.
(2) The most effective designs of aluminum body can be made through the integration of multi-criteria optimization and Pareto-optimal sensitivity under the given various structural specifications and constraints based

on the design parameter screening process.

(3) This simulation procedure provides an efficient design for many mechanical structures in the early stages of their development.

References

(1) Lee, D. C. and Lee, J. I., 2003, "A structural optimization design for aluminum-intensive vehicle," *Proc. Instn. Mech. Engrs, Part D; Journal of Automobile Engineering*, 2003, Vol. 217, No. 9, pp. 771~779.

(2) Ingo, R., 2004, "Sizing in conceptual design at BMW," *SAE 2004-01-1657.*

(3) Yasuaki, T., 2004, "First-order analysis for automotive body structure design-Part 2: Joint analysis considering nonlinear behavior," *SAE 2004-01-1659.*

(4) Hidekazu, N. and Noboru, K., 2004, "First-order analysis for automotive body structure design-Part 3: crashworthiness analysis using beam elements," *SAE 2004-01-1660.*

(5) Toshiaki, N., 2004, "First-order analysis for automotive body structure design-Part 4: Noise and vibration analysis applied to a subframe," *SAE 2004-01-1661.*

(6) Lee, D. C., 2004, "A design of panel structure for the improvement of dynamic stiffness," *Proc. Instn. Mech. Engrs, Part D; Journal of Automobile Engineering*, Vol. 218, No. 6, pp. 647~654.

(7) Lee, D. C., Choi, H. S., and Han, C. S., 2006, "Design of automotive body structure using multicriteria optimization," *Struct. Multidisc. Optim.*, Vol. 32, No. 2, pp. 161~167.

(8) Wierzbicki, T. and Abramowicz, W., 1983, "On the Crushing Mechanics of Thin-Walled Structures," *J. Appl. Mech.*, Vol. 50, No. 4, pp. 727~734.

(9) Kecman, D., 1983, "Bending Collapse of Rectangular and Square Section Tubes," *Int. J. Mech. Sci.*, Vol. 25, No. 9, pp. 623~636.

(10) Hong, S. J., Lee, D. C., Jang, J. H., Han, C. S., and Hedrick, K., 2006, "Systematic design process for frontal crashworthiness of aluminum-intensive electrical vehicle bodies," *Proc. Instn. Mech. Engrs, Part D; Journal of Automobile Engineering*, Vol. 220, No. 12, pp. 1667~1678.

(11) Shawn, R. D., Ghassan, T. K., and Roger, C. S., 2005, "Design and analysis of a conceptual modular aluminum spaceframe platform," *SAE 2005-01-1029.*

(12) Lee, K. H., Lee, G. H., Bae, I. H., and Chong, T. H., 2007, "An optimum design method of hypoid gear by minimizing volume," *Transactions of the Korean Society of Machine Tool Engineering*, Vol. 16, No. 6, pp. 55~61.

(13) Kim, H. G., Nah, S. C., Hong, D. P., and Cho, N. I., 2007, "A study on the optimal design for aluminium boom shape in high ladder vehicles," *Transactions of the Korean Society of Machine Tool Engineering*, Vol. 16, No. 3, pp. 96~102.